The 3D model of the plasmasphere coupled to the ionosphere

V. Pierrard[1,2] and M. Voiculescu[3]

Received 12 April 2011; revised 13 May 2011; accepted 13 May 2011; published 25 June 2011.

[1] The 3D dynamic model of the plasmasphere developed by Pierrard and Stegen (2008) has been coupled with the ionospheric IRI model. In addition to the electron number density, the plasmaspheric model is also developed to include the temperature profiles of the different particles and ion composition at altitudes from 60 to 2000 km. Results of the model for the F region trough are compared with coincident observations of middle and top ionosphere by means of satellite tomography and radar measurements. A good match between the model and observations supports the idea that the present model is useful for investigating physical mechanism involved in the plasmasphere-ionosphere coupling and for acquiring information about the plasmaspheric behaviour based on ionospheric observations. **Citation:** Pierrard, V., and M. Voiculescu (2011), The 3D model of the plasmasphere coupled to the ionosphere, *Geophys. Res. Lett.*, *38*, L12104, doi:10.1029/2011GL047767.

1. Introduction

[2] A three dimensional dynamic model of the plasmasphere has recently been developed by *Pierrard and Stegen* [2008]. This physics-based model uses the kinetic approach to determine the number density of the electrons inside and outside the plasmasphere and the position of the plasmapause as a function of the geomagnetic activity level index Kp. The authors showed that the plasmasphere is a highly dynamic region and presents different features depending on the geomagnetic activity. During quiet periods, the plasmasphere is extended to radial distances larger than 4 Re. During geomagnetic storms and substorms, the plasmasphere is eroded and a sharp plasmapause forms closer to the Earth (see *Goldstein* [2006] for a review) [*Lemaire and Pierrard*, 2008]. Plumes are then formed in the afternoon MLT sector and rotate with the Earth [*Spasojević et al.*, 2003; *Pierrard and Lemaire*, 2004; *Darrouzet et al.*, 2006]. The results of the model have been compared to recent observations of Cluster and IMAGE [*Pierrard and Cabrera*, 2005, 2006; *Pierrard*, 2006; *Darrouzet et al.*, 2009] and have shown that the model globally reproduces the dynamic features of the plasmasphere.

[3] In the present work, temperatures and ion composition have been added to improve and extend the model. Moreover, the model has been coupled with an ionospheric model that gives the number density and temperatures of the different particles at altitudes from 60 to 2000 km. We use here the IRI model [*Bilitza and Reinisch*, 2008], but other ionospheric models can be used as well. The International Reference Ionosphere (IRI) is an empirical standard model of the ionosphere, based on all available data sources. For a given location, time and date, IRI calculates the electron density, electron temperature, ion temperature, and ion composition in the altitude range from 60 km to 2000 km, and also the total electron content. Several steadily improved editions of the model have been released [*Bilitza*, 2001; *Bilitza and Reinisch*, 2008; *Richards et al.*, 2010]. The IRI Fortran software can be obtained from the solar-terrestrial models archive of NASA's Space Physics Data Facility and National Space Science Data Center at http:/nssdcftp/models/ionospheric/iri/iri2007/. A web interface for computing and plotting IRI values is accessible from the IRI homepage at http://IRI.gsfc.nasa.gov. The ionospheric composition and temperatures obtained with the ionospheric model are used as boundary conditions in the physics-based model of the plasmasphere. Since the plasmasphere is the extension of the ionosphere at low and middle latitudes, a coupled model is really necessary for a better understanding of the interplay between the ionosphere and the plasmasphere. These regions play an important role for technological systems and have impact for navigation, communication and radar observations. The ionosphere-plasmasphere model gives temporal evolution of the electron density that can be compared with the Total Electron Content observed by the Global Positioning System (GPS). Moreover, the plasmaspheric region populated by cold plasma from the ionosphere has direct influence on other regions of the magnetosphere. For instance radiation belt energetic particle populations, which are crucial for spacecraft missions and for the health of the astronauts, are very sensitive to the core plasmasphere distribution, specifically to the position of the plasmapause.

[4] The position of the plasmapause and the associated gradient densities at the plasmapause are related to the ionospheric trough [e.g., *Rycroft and Burnell*, 1970]. Coincident observations of the middle and top ionosphere using satellite tomography, and plasmapause observations have been used to test the model for the capabilities of reproducing the ionospheric F region trough.

2. Extension of the Model to Ion Composition and Temperatures

2.1. Number Density Profiles

[5] The physics-based plasmaspheric model determines the number density and other moments of the particles with a kinetic Vlasov code [*Pierrard and Stegen*, 2008]. The particles are submitted to the effects of the external forces, i.e., the gravitational attraction, the electric force and the Lorentz force due to the magnetic field. In the model

[1]Belgian Institute for Space Aeronomy, Brussels, Belgium.
[2]Center for Space Radiations, Institute of Research in Mathematics and Physics, Université Catholique de Louvain, Louvain-La-Neuve, Belgium.
[3]Faculty of Sciences and Environment, Dunarea de Jos University of Galati, Galati, Romania.

Copyright 2011 by the American Geophysical Union.
0094-8276/11/2011GL047767

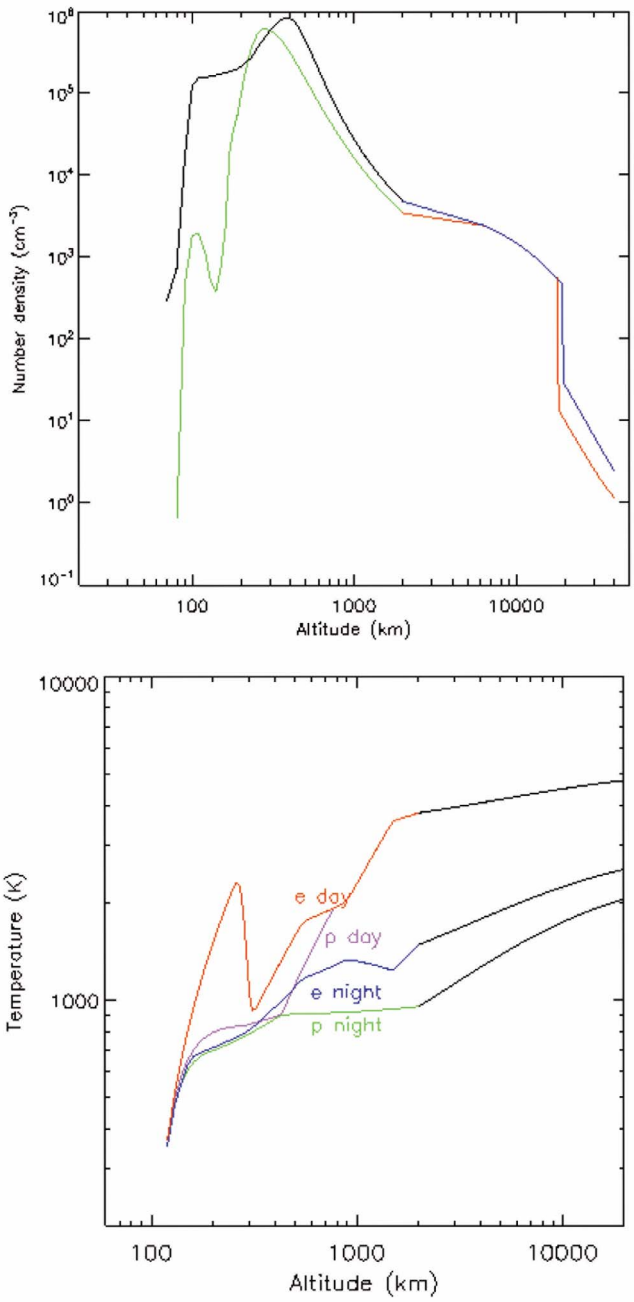

Figure 1. (top) Electron density predicted by the plasmaspheric model coupled with IRI at ionospheric altitudes for an example date chosen to be 28 Sept. 2005. At 0 MLT (midnight), IRI is illustrated in green and the plasmaspheric extension in red. The plasmapause limit and the plasmaspheric trough correspond to the sharp decrease at about 18.000 km (3.8 Re) and the low density region outside the plasmasphere. At 12 MLT, IRI is illustrated in black and the plasmasphere/trough in blue. (bottom) Temperatures of the protons (and other ions) and electrons in the IRI model of the ionosphere (colored lines) and in the model of the plasmasphere (black lines) in the geomagnetic equatorial plane during night (0 MLT) and day (12 MLT) on 28 September 2005.

described in the present paper, the flux of particles circulates from one hemisphere to the other, so that the net flux is equal to zero. Nevertheless, the model can also be used in the case of an external flux considering a plasmaspheric wind [*André and Lemaire*, 2006]. To determine the composition and the temperature of the plasma in the plasmasphere, we use as boundary conditions the proportion of ions and the temperatures of the particles obtained with the IRI model at 2000 km [*Bilitza and Reinisch*, 2008]. The number density of the different particle species inside the plasmasphere is dependent on the ionospheric conditions. The ionospheric model IRI and thus the plasmaspheric densities and temperatures depend on the date, the daily solar radio flux $F_{10.7}$ [10^{-22} W m^{-2} Hz^{-1}], the sunspot number (12 months average) as well as on the position (altitude, latitude, and local time associated to the longitude). The solar activity has thus an influence on the number density of the electrons in the coupled model: it is slightly lower during solar minimum than during solar maximum.

[6] Coupling the plasmaspheric model with another ionospheric empirical or physics-based model is, of course, also possible. The ionospheric model has to determine the number density of the different particle species and their temperatures up to 2000 km so that the profiles can be extended to the plasmasphere with the dynamic model. The results of our coupled model are illustrated in Figure 1 (top) that presents in logarithmic scale the number density of the electrons obtained at 28 Sept. 2005 at 12 MLT (day) and 0 MLT (night) in the geomagnetic equatorial plane.

[7] As illustrated in Figure 1, the magnetic local time plays an important role in the density variations in the different regions, i.e., in the ionosphere, the plasmasphere and the region outside the plasmasphere called the plasmaspheric trough as well as on the position of the plasmapause. The number densities are generally higher at 12 MLT than at 0 MLT. The effect of MLT on the density is especially high in the ionosphere. The accuracy of the low altitude plasmaspheric number density is thus crucial, especially for comparison with empirical models based on GPS TEC models [*Heise et al.*, 2002]. The MLT modulation of the number density is weaker inside the plasmasphere and is generally neglected in plasmaspheric models (see *Carpenter and Anderson* [1992], *Gallagher et al.* [2000], and *Reinisch et al.* [2009] for a review).

[8] The plasmaspheric density at large radial distances, i.e., in the plasmatrough, is also highly variable and depends on the MLT sector and on the position of the plasmapause determined by the Kp variations during the previous 24 hours. In our dynamic model, the plasmapause is determined by the mechanism of interchange instability [*Lemaire and Pierrard*, 2008]. This instability appears at radial distances where the centrifugal force becomes larger than the gravitational force, called the Zero Parallel Force Surface [*Pierrard and Lemaire*, 2004]. Kp describes the geomagnetic activity, whose level determines the convection electric field that is dominant at large radial distances. We use the empirical model E5D [*McIlwain*, 1986] combined with the corotation electric field. Other electric field models can be used as well [*Pierrard et al.*, 2008]. Above the plasmapause (illustrated on Figure 1 by the sharp decreases of the number density at altitudes around 19000 km, i.e., about 4 Re in radial distances, depending on MLT and Kp variations) the number density in the plasmatrough is also MLT-dependent.

[9] The coupled model gives not only the electron number density, but also the number densities of each ion species, especially O^+, N^+, H^+, He^+, O_2^+ and NO^+ that vary with the altitude. Heavy ions dominate in the low ionosphere, but at 2000 km and above, the major species are generally the light H^+ ions and He^+ ions. The other ions are generally negligible but their proportion depends on the temperature and geomagnetic activity. The proportion of Helium ions above 2000 km depends on ionospheric conditions. In our example, the ion composition given by IRI2008 at 2000 km at this specific date is 58,1% of H^+ and 41.9% of He^+.at 12 MLT (dayside). At 0 MLT (midnight), the percentage of H^+ is 95%, He^+ represents 3.9% of the ion density and O^+ 0.9%. The Helium proportion is observed to be 8% in average inside the plasmasphere [*Dandouras et al.*, 2005].

2.2. Extension of the Model to Temperature Profiles

[10] The IRI ionospheric model determines the temperatures of the electrons and ions from 60 up to 2000 km of altitude. These values are used as boundary conditions to obtain the temperature profiles in the plasmasphere with the kinetic model. Figure 1 (bottom) illustrates the temperature profiles given by IRI for the date of 28 September 2005 from 120 km to 2000 km: the red line corresponds to the electron temperature at 12 MLT, the magenta line to the proton (and other ions) temperature at 12 MLT, the blue line represents the electron temperature at 0 MLT and the green line corresponds to the proton (and other ions) temperature at 0 MLT. Black lines correspond to the temperature profiles obtained with the plasmaspheric model above 2000 km. All the ions are assumed in thermal equilibrium in the IRI model and thus in the plasmaspheric model as well. The temperature of the electrons, on the other hand, is different from the ion one, especially during the night and at high altitudes, as shown in Figure 1.

[11] The temperature profiles in the plasmasphere are obtained by using the kinetic model developed by *Pierrard and Lemaire* [2001]. Assuming that the plasmaspheric particles have velocity distribution functions with suprathermal tails as generally observed in space plasmas, the temperature increases as a function of the radial distance by velocity filtration effect (see *Pierrard and Lazar* [2010] for a review). Such distributions are well represented by Kappa functions, where the parameter kappa is here chosen to be $\kappa = 2$ to obtain the most realistic temperatures compared to satellite observations in the plasmasphere. *Comfort* [1986] determined plasmaspheric thermal structure from a statistical survey of low-energy (<50 eV) ions measured by the Retarding Ion Mass Spectrometer (RIMS) on the DE-1 satellite. Typical dayside temperatures range from about 4000 K in the inner plasmasphere to over 10000 K in the outer plasmasphere, while corresponding evening side temperatures range from near 2000 K to over 10000 K. *Bezrukikh et al.* [2003] have also measured the temperatures of plasmaspheric protons with the Auroral Probe Alpha3 instrument: they found protons temperatures between 1300 and 7000 K depending on the MLT (night or day) and on geomagnetic conditions (quiet or disturbed). The temperature increases in the ionosphere and continues to increase at higher altitudes, in the plasmasphere. Temperatures are clearly higher during day than during night as illustrated by Figure 1 (bottom). The coupled model allows also studying the interactions with the thermosphere. IRI gives the temperature of the neutral particles, based on the MSIS empirical model of *Hedin* [1991] providing complete thermospheric temperatures and densities based on in-situ data from seven satellites and numerous rocket probes. The IRI temperature of neutral particles in our example is 712 K (0 MLT) and 834 K (12 MLT) at 2000 km of altitude. The number density of the neutral particles is large in the middle ionosphere but decreases fast with altitude, reaching 6 10^4 hydrogen atoms/cm^{-3} at 2000 km at 0 MLT in our example. At high altitudes, hydrogen is the main species of neutral particles, followed by a small amount of helium (around 10% at 2000 km).

3. The Link Between the Plasmapause and the Ionospheric Trough

[12] In their pioneer works, *Rycroft and Burnell* [1970] and *Rycroft and Thomas* [1970] have established statistically a direct relation between the plasmapause and the ionospheric trough between 21 and 5 local time. More recently, *Grebowsky et al.* [2009] have shown that statistically, the signature of the plasmapause coincides with the main ionospheric electron density trough at night. One should note, however, that the plasmapause is a boundary with a narrow extent, while the ionospheric trough has widths that vary from 1–2 degrees to 10 degrees or even more. Thus the main trough, classically considered as the separator between the mid-latitudinal ionosphere and the auroral precipitation, should correspond to the plasmatrough, which separates the plasmasphere from the magnetosheet. Some studies have been more precise in specifying that the ionospheric projection of the plasmapause falls close to the equatorward wall [*Yizengaw et al.*, 2005; *Yizengaw and Moldwin*, 2005]. When the plasmapause goes closer to the Earth during geomagnetic storms, its projection in the ionosphere is located at lower latitudes and this is observed for the ionospheric trough as well [e.g., *Voiculescu et al.*, 2006, and references therein].

[13] The plasmapause, i.e., the associated phenomena (turbulence and instabilities), can induce some modifications in the top ionosphere, which can be useful in evaluating the position of the plasmapause from ionospheric measurements with an accuracy of about 2–3 deg [*Titheridge*, 1976]. The plasmapause position is associated with the ionospheric latitude where electron temperature increases, concentration of H^+ is rapidly increasing or with the lowest latitude where the ion transition altitude does not vary. The best localization of the plasmapause from ionospheric measurements seems to be obtained when all three processes occur at the same latitude. The light ion trough (LIT) forming in the top ionosphere is another phenomenon which is associated to the plasmapause [*Taylor and Walsh*, 1972] although it has been shown that LIT forms actually several degrees equatorward from the plasmapause projection [*Foster et al.*, 1978].

[14] Figure 2 illustrates the position of the plasmapause and the number density of the electrons inside the plasmasphere as given by the model on 28 September 2005 at 18:30 UT in the geomagnetic equatorial plane for the different MLT sectors. The Sun (12 MLT) is on the left side of Figure 2. In our example, Kp is only slightly varying, so that

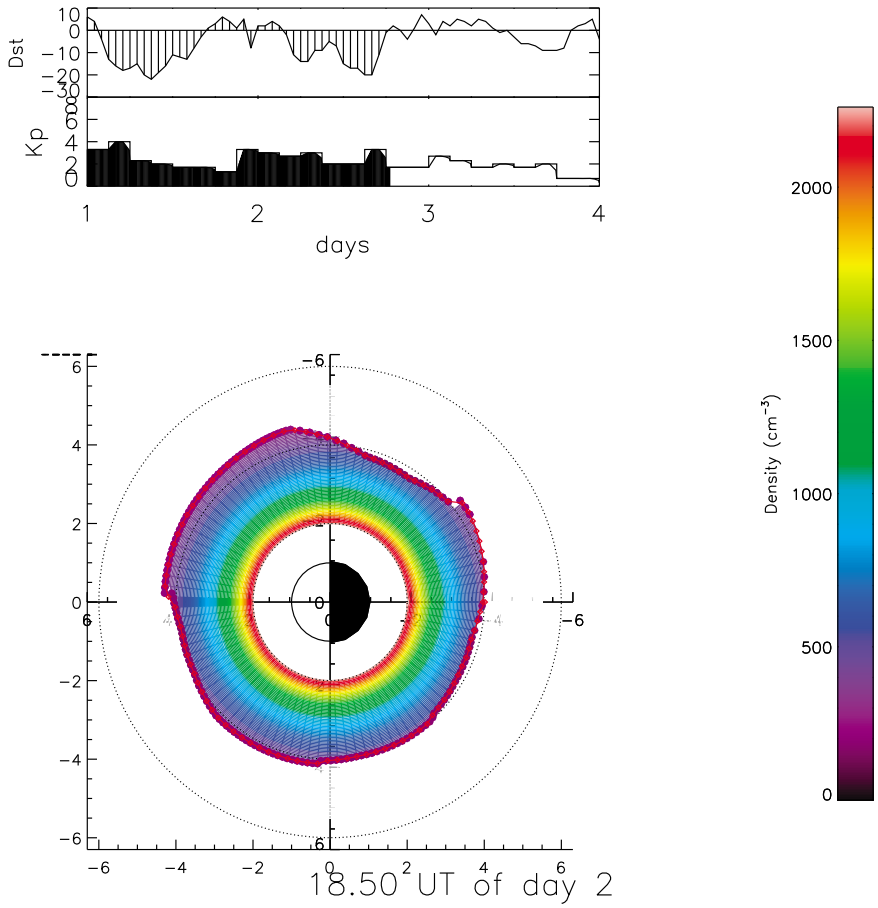

Figure 2. Number density of the electrons in the plasmasphere and position of the plasmapause given by the model on 28 September 2005, 18:30 UT, in the geomagnetic equatorial plane.

the plasmapause is around 4 Re at each MLT sector (more exactly at 4 for 12 MLT and 3.8 at 0 MLT).

[15] Figure 3 shows observations of the ionospheric trough by means of satellite tomography [e.g., *Nygrén et al.*, 1997] on 28 Sept. 2005 at 18:36 UT, 20:35 MLT (middle panel) together with coincident observations of the DMSP satellites of the density and temperatures in the top ionosphere (upper panels). A very good correspondence is observed between the trough observed both in the top ionosphere and F region. Figure 3 (bottom) illustrates the result of the coupled model at the same time and MLT sector (spatial distribution of electron density and vertical variation of number density at different latitudes). In our coupled model, we consider that a link exists between the plasmapause and the ionospheric trough by assuming that the same geomagnetic field line connects the plasmapause and the ionospheric equatorward wall of the trough. The number density of the ionospheric electrons below the plasmapause latitudes is obtained from the IRI model.

[16] In this example, the observed ionospheric trough is nicely reproduced by the model. The modeled plasmapause projects in the ionosphere at magnetic latitude of 59°, which coincides with the location of the equatorward wall of the observed ionospheric trough both in the F region and in the top ionosphere. Moreover, the variation of the plasma density with latitude and altitude is also reasonably well reproduced. Both in the model and in the tomographic observation, h_{max} is about 300 km.

[17] The electron density is higher in the model than in the observations. This can be due to the fact that the tomographic reconstruction underestimates the peak densities [*Nygrén et al.*, 1996]. An overestimation of the plasma densities in the ionosphere by the model is also possible. Note also that IRI is a climatological model representing monthly average conditions, so differences to a specific day are not surprising.

[18] One cannot expect a perfect match of the plasmapause with the ionospheric trough because the latter is more complex since part of the processes contributing to the formation of the ionospheric trough are local and unrelated to electromagnetic forces (winds, neutral turbulence, neutral waves). Thus it is likely that the coincidence between plasmapause and ionospheric trough is valid only for particular conditions, more precisely when the ionospheric trough forms as a consequence of global mechanisms. When the ionospheric trough is the result of neutral upwelling due, for instance, to local heating, the coincidence is less likely to occur.

[19] Despite missing data in temperature and density profiles for the top ionosphere, Figure 3 shows that the

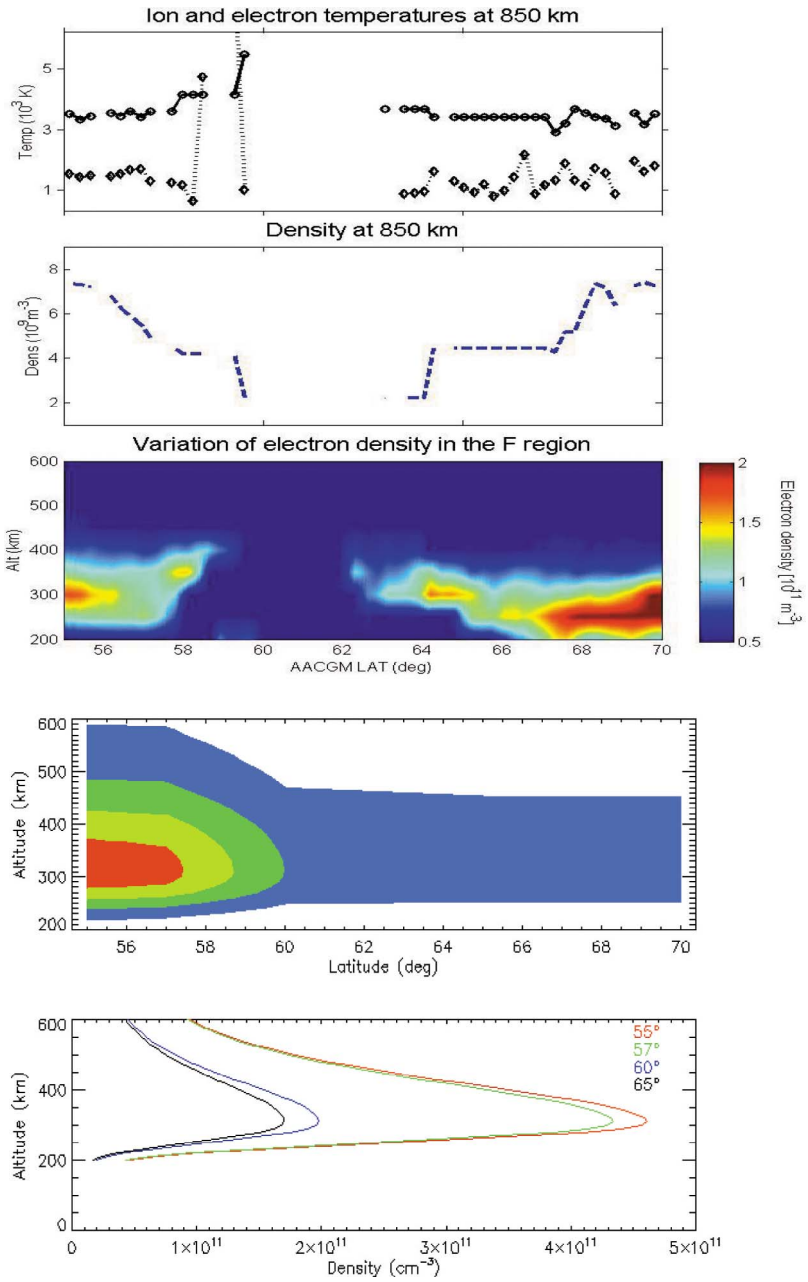

Figure 3. (top and middle top) Ion (open diamonds) and electron temperatures (open circles) and electron density in the top ionosphere, at 850 km. (middle) Ionogram of the F region ionosphere obtained by satellite tomography (courtesy to Tero Raita, Sodankyla Geophysical Observatory, Finland) on 28 September 2005 (18:36 UT, 20:35 MLT). (middle bottom and bottom) Ionogram of the F region ionosphere obtained from the dynamic model of the plasmasphere coupled with the ionosphere and number density of ionospheric electrons deduced from the coupled model as a function of the altitude and for different latitudes.

plasmapause coincides with some increases in electron temperature, as predicted by some authors [*Green et al.*, 1986] and confirmed by other observations [*Afonin et al.*, 1997]. Such an increase of the temperature at the plasmapause is also obtained in our model due to the different origin of the plasmatrough plasma. The high ion temperatures observed in the outer plasmasphere flux tubes during refilling conditions were also reproduced by the hydrodynamic model of *Comfort et al.* [1995] with modified thermal conductivity coefficients.

4. Conclusions

[20] The plasmaspheric model developed by *Pierrard and Stegen* [2008] has been coupled with the ionospheric IRI model to provide the number density and the temperatures

of the electrons and ions from the lowest ionospheric altitudes to the largest plasmatrough radial distances. This allows us to better study the dynamics of the thermosphere/ionosphere/plasmasphere system and the links between the ionospheric trough and the plasmapause. In order to test the validity of the coupled model, the ionogram obtained by projecting model results into the ionosphere has been compared with tomographic and satellite observations. A good agreement has been found between observations and model results, showing that the plasmapause corresponds to the equatorward wall of the ionospheric trough for quiet conditions.

[21] The projection of the plasmapause can be related to the ionospheric trough for normal conditions during quiet ionosphere and moderately disturbed periods. The correlation should be mainly valid at night time, because in the daytime, photoionization and magnetic field aligned diffusion dominates the latitudinal distribution of the electrons in the F region. Moreover, the morphology of the ionospheric trough is more complex since it is driven also by other processes as well, as for instance local chemical processes, neutral wind-drag, local effects of high local electric fields, thus the projection of the modeled plasmapause into the ionosphere might not coincide always with the trough. Coincident in situ measurements of the plasmasphere and the ionosphere are necessary to improve the results of the analysis. However, our results show that the model can be used for investigating more thoroughly the link between the ionospheric trough and plasmapause.

[22] Compared with other existing plasmaspheric models (see *Pierrard et al.* [2009] for a review), our coupled model is especially dedicated to a better 3D visualization of the dynamics of the ionosphere-plasmasphere system aiming at a better understanding of the mechanisms influencing the ionosphere-magnetosphere interactions. Features of the ionosphere (as for instance, the trough) can be reproduced, which means that the model can be used to infer plasmaspheric features based on ionospheric observations. In the future, the same kinetic approach will also be used to model the polar wind escaping at high latitudes along open field lines [*Tam et al.*, 2007].

[23] **Acknowledgments.** This research has received funding from the European Commission's FP7 Program inside the grant agreement SWIFF (project 2633430, swiff.eu). V. Pierrard and M. Voiculescu thank the Solar-Terrestrial Center of Excellence for the support. Project 81-009/SAFIR of the Romanian National Plan for Research, Development and Innovation is acknowledged. We gratefully acknowledge the Center for Space Sciences at the University of Texas at Dallas and the US Air Force for providing the DMSP thermal plasma data. The Scandinavian tomography chain is run by Sodankyl at Geophysical Observatory, Finland. We are grateful to T. Raita and J. Manninen for their continuous effort in maintaining the receiver chain and for providing tomographic data.

[24] The Editor thanks Dennis Gallagher and Dieter Bilitza for their assistance in evaluating this paper.

References

Afonin, V. V., V. S. Bassolo, J. Smilauer, and J. F. Lemaire (1997), Motion and erosion of the nightside plasmapause region and of the associated subauroral electron temperature enhancement: Cosmos 900 observations, *J. Geophys. Res.*, *102*(A2), 2093–2103, doi:10.1029/96JA02497.

André, N., and J. F. Lemaire (2006), Convective instabilities in the plasmasphere, *J. Atmos. Sol. Terr. Phys.*, *68*(2), 213–227, doi:10.1016/j.jastp.2005.10.013.

Bezrukikh, V. V., G. A. Kotova, L. A. Lezhen, J. Lemaire, V. Pierrard, and Y. I. Venediktov (2003), Dynamics of temperature and density of cold protons of the Earth's plasmasphere measured by the Auroral Probe/Alpha-3 experiment data during geomagnetic disturbances, Cosmic Res., *Engl. Transl.*, *41*(4), 392–402, doi:10.1023/A:1025013828230.

Bilitza, D. (2001), International Reference Ionosphere 2000, *Radio Sci.*, *36*, 261–275, doi:10.1029/2000RS002432.

Bilitza, D., and B. Reinisch (2008), International Reference Ionosphere 2007: Improvements and new parameters, *Adv. Space Res.*, *42*(4), 599–609, doi:10.1016/j.asr.2007.07.048.

Carpenter, D. L., and R. R. Anderson (1992), An ISEE/Whistler model of equatorial electron density in the magnetosphere, *J. Geophys. Res.*, *97*, 1097–1108, doi:10.1029/91JA01548.

Comfort, R. H. (1986), Plasmasphere thermal structure as measured by ISEE-1 and DE-1, *Adv. Space Res.*, *6*(3), 31–40, doi:10.1016/0273-1177(86)90314-5.

Comfort, R. H., P. D. Craven, and P. G. Richards (1995), A modified thermal conductivity for low density plasma magnetic flux tubes, *Geophys. Res. Lett.*, *22*(18), 2457–2460, doi:10.1029/95GL02408.

Dandouras, I., et al. (2005), Multipoint observations of ionic structures in the Plasmasphere by CLUSTER-CIS and comparisons with IMAGE-EUV observations and with Model Simulations, in *Inner Magnetosphere Interactions: New Perspectives from Imaging*, *Geophys. Monogr. Ser.*, vol. 159, edited by J. L. Burch, M. Schultz, and H. Spence, pp. 23–54, AGU, Washington, D. C.

Darrouzet, F., et al. (2006), Analysis of plasmaspheric plumes: CLUSTER and IMAGE observations, *Ann. Geophys.*, *24*, 1737–1758, doi:10.5194/angeo-24-1737-2006.

Darrouzet, F., J. De Keyser, and V. Pierrard (Eds.) (2009), *The Earth's Plasmasphere: Cluster and IMAGE—A Modern Perspective*, 296 pp., Springer, New York.

Foster, J. C., C. G. Park, L. H. Brace, J. R. Burrows, J. H. Hoffman, E. J. Maier, and J. H. Whitteker (1978), Plasmapause signatures in the ionosphere and magnetosphere, *J. Geophys. Res.*, *83*(A3), 1175–1182, doi:10.1029/JA083iA03p01175.

Gallagher, D. L., P. D. Craven, and R. H. Comfort (2000), Global core plasma model, *J. Geophys. Res.*, *105*(A8), 18,819–18,833, doi:10.1029/1999JA000241.

Goldstein, J. (2006), Plasmasphere response: Tutorial and review of recent imaging results, *Space Sci. Rev.*, *124*(1–4), 203–216, doi:10.1007/s11214-006-9105-y.

Grebowsky, J. M., R. F. Benson, P. A. Webb, V. Truhlik, and D. Bilitza (2009), Altitude variation of the plasmapause signature in the main ionospheric trough, *J. Atmos. Sol. Terr. Phys.*, *71*, 1669–1676, doi:10.1016/j.jastp.2009.05.016.

Green, J. L., et al. (1986), Observations of ionospheric magnetospheric coupling: DE and Chatanika coincidences, *J. Geophys. Res.*, *91*(A5), 5803–5815, doi:10.1029/JA091iA05p05803.

Hedin, A. E. (1991), Extension of the MSIS thermosphere model into the middle and lower atmosphere, *J. Geophys. Res.*, *96*(A2), 1159–1172, doi:10.1029/90JA02125.

Heise, S., N. Jakowski, A. Wehrenpfennig, C. Reigber, and H. Lühr (2002), Sounding of the topside ionosphere/plasmasphere based on GPS measurements from CHAMP: Initial results, *Geophys. Res. Lett.*, *29*(14), 1699, doi:10.1029/2002GL014738.

Lemaire, J., and V. Pierrard (2008), Comparison between two theoretical mechanisms for the formation of the plasmapause and relevant observations, *Geomagn. Aeron., Engl. Transl.*, *48*(5), 553–570, doi:10.1134/S0016793208050010.

McIlwain, C. E. (1986), A Kp dependent equatorial electric field model, *Adv. Space Res.*, *6*(3), 187–197, doi:10.1016/0273-1177(86)90331-5.

Nygrén, T., M. Markkanen, M. Lehtinen, E. D. Tereshchenko, B. Z. Khudukon, O. V. Evstafiev, and P. Pollari (1996), Comparison of F-region electron density observations by satellite radio tomography and incoherent scatter methods, *Ann. Geophys.*, *14*, 1422–1428.

Nygrén, T., M. Markkanen, M. Lehtinen, E. D. Tereshchenko, and B. Z. Khudukon (1997), Stochastic inversion in ionospheric radiotomography, *Radio Sci.*, *32*, 2359–2372, doi:10.1029/97RS02915.

Pierrard, V. (2006), The dynamics of the plasmasphere, in *Space Science: New Research*, edited by Nick S. Maravell, pp. 83–96, Nova Sci., New York.

Pierrard, V., and J. Cabrera (2005), Comparisons between EUV/IMAGE observations and numerical simulations of the plasmapause formation, *Ann. Geophys.*, *23*, 2635–2646, doi:10.5194/angeo-23-2635-2005.

Pierrard, V., and J. Cabrera (2006), Dynamical simulations of plasmapause deformations, *Space Sci. Rev.*, *122*(1–4), 119–126, doi:10.1007/s11214-006-5670-3.

Pierrard, V., and M. Lazar (2010), Kappa distributions: Theory and applications in space plasmas, *Sol. Phys.*, *267*(1), 153–174, doi:10.1007/s11207-010-9640-2.

Pierrard, V., and J. Lemaire (2001), Exospheric model of the plasmasphere, *J. Atmos. Sol. Terr. Phys.*, *63*(11), 1261–1265, doi:10.1016/S1364-6826(00)00227-3.

Pierrard, V., and J. F. Lemaire (2004), Development of shoulders and plumes in the frame of the interchange instability mechanism for plasmapause formation, *Geophys. Res. Lett.*, *31*, L05809, doi:10.1029/2003GL018919.

Pierrard, V., and K. Stegen (2008), A three dimensional dynamic kinetic model of the plasmasphere, *J. Geophys. Res.*, *113*, A10209, doi:10.1029/2008JA013060.

Pierrard, V., G. Khazanov, J. Cabrera, and J. Lemaire (2008), Influence of the convection electric field models on predicted plasmapause positions during the magnetic storms, *J. Geophys. Res.*, *113*, A08212, doi:10.1029/2007JA012612.

Pierrard, V., J. Goldstein, N. André, V. K. Jordanova, G. A. Kotova, J. F. Lemaire, M. W. Liemohn, and H. Matsui (2009), Recent progress in physics-based models of the plasmasphere, *Space Sci. Rev.*, *145*(1–2), 193–229, doi:10.1007/s11214-008-9480-7.

Reinisch, B. W., M. B. Moldwin, R. E. Denton, D. L. Gallagher, H. Matsui, V. Pierrard, and J. Tu (2009), Augmented Empirical models of the plasmaspheric density and electric field using IMAGE and CLUSTER data, *Space Sci. Rev.*, *145*(1–2), 231–261, doi:10.1007/s11214-008-9481-6.

Richards, P. G., D. Bilitza, and D. Voglozin (2010), Ion density calculator (IDC): A new efficient model of ionospheric ion densities, *Radio Sci.*, *45*, RS5007, doi:10.1029/2009RS004332.

Rycroft, M. J., and S. J. Burnell (1970), Statistical analysis of movements of the ionospheric trough and the plasmapause, *J. Geophys. Res.*, *75*(28), 5600–5604, doi:10.1029/JA075i028p05600.

Rycroft, M. J., and J. O. Thomas (1970), The magnetospheric plasmapause and the electron density trough at the Alouette I orbit, *Planet. Space Sci.*, *18*, 65–80, doi:10.1016/0032-0633(70)90067-X.

Spasojević, M., J. Goldstein, D. L. Carpenter, U. S. Inan, B. R. Sandel, M. B. Moldwin, and B. W. Reinisch (2003), Global response of the plasmasphere to a geomagnetic disturbance, *J. Geophys. Res.*, *108*(A9), 1340, doi:10.1029/2003JA009987.

Tam, S. W. Y., T. Chang, and V. Pierrard (2007), Kinetic modeling of the polar wind, *J. Atmos. Sol. Terr. Phys.*, *69*(16), 1984–2027, doi:10.1016/j.jastp.2007.08.006.

Taylor, H. A., Jr., and W. J. Walsh (1972), The light ion trough, the main trough and the plasmapause, *J. Geophys. Res.*, *77*(34), 6716–6723, doi:10.1029/JA077i034p06716.

Titheridge, J. (1976), Plasmapause effects in the top side ionosphere, *J. Geophys. Res.*, *81*(19), 3227–3233, doi:10.1029/JA081i019p03227.

Voiculescu, M., I. Virtanen, and T. Nygrén (2006), The F region ionospheric trough: Seasonal dependence and relation to IMF, *Ann. Geophys.*, *24*(1), 173–185, doi:10.5194/angeo-24-173-2006.

Yizengaw, E., and M. B. Moldwin (2005), The altitude extension of the mid-latitude trough and its correlation with plasmapause position, *Geophys. Res. Lett.*, *32*, L09105, doi:10.1029/2005GL022854.

Yizengaw, E., H. Wei, M. B. Moldwin, D. Galvan, L. Mandrake, A. Mannucci, and X. Pi (2005), The correlation between mid-latitude trough and the plasmapause, *Geophys. Res. Lett.*, *32*, L10102, doi:10.1029/2005GL022954.

V. Pierrard, Belgian Institute for Space Aeronomy, 3 av. Circulaire, B-1180 Brussels, Belgium. (viviane.pierrard@oma.be)

M. Voiculescu, Faculty of Sciences and Environment, Dunarea de Jos University of Galati, 111 Domneasca Str., Galati 800201, Romania.